PII: S0032-3861(98)00065-2

# Investigation of glass transition behaviours in aromatic poly(amic acid) precursors with various chain rigidities by oscillating differential scanning calorimetry

**S.I. Kim, S.M. Pyo, K. Kim and M. Ree\***
*Department of Chemistry and Polymer Research Institute, Pohang University of Science and Technology, San 31, Hyoja-dong, Pohang 790-784, South Korea*
*(Received 7 November 1997; revised 22 December 1997; accepted 16 January 1998)*

Most aromatic poly(amic acid)s, which are precursor polymers of polyimides, are thermally converted to the corresponding polyimides via imide-ring closure formation over their glass transition temperature ($T_g$) ranges or below. In addition, it is very difficult to remove completely solvents used in the synthesis from their cast samples, due to the formation of complexes between the solvent molecules and the orthoamic acid groups in poly(amic acid)s. For these reasons, it is not possible to measure $T_g$ values of poly(amic acid)s with residual solvent or of poly(amic acid)s with solvent free in conventional ways. However, in the present study $T_g$ values of several poly(amic acid)s were successfully measured as a function of the content of residual solvent by the recently developed oscillating differential scanning calorimetry: poly(*p*-phenylene biphenyltetracarboxamic acid) (BPDA-PDA), poly(*p*-phenylene pyromellitamic acid) (PMDA-PDA), and poly(4,4′-oxydiphenylene biphenyltetra-carboxamic acid) (BPDA-ODA) precursors. The content of residual solvent in cast poly(amic acid) samples was independently determined by proton nuclear magnetic resonance spectroscopy. By fitting the measured $T_g$ values by a modified Gordon–Taylor equation as a function of composition, $T_g$ values of the poly(amic acid)s in solvent free were estimated: 248.4°C for BPDA-PDA, 283.4°C for PMDA-PDA, and 184.4°C for BPDA-ODA precursor. The estimated $T_g$ values were correlated to the calculated Kuhn statistical segments ($L_K$ values), which are the measures of chain rigidities: 62.2 Å for BPDA-PDA, 88.7 Å for PMDA-PDA, and 41.2 Å for BPDA-ODA: That is, high chain rigidity causes higher $T_g$. In addition, phase diagrams of the poly(amic acid)/*N*-methyl-2-pyrrolidone solvent mixtures were constructed. The number of solvent molecules bound to the chemical repeat unit were also estimated to be 1.46–2.16 in the highly dried precursors, depending on the poly(amic acid)s. © 1998 Published by Elsevier Science Ltd. All rights reserved.

(Keywords: poly(amic acid)s; polyimide; glass transition temperature)

## INTRODUCTION

Aromatic polyimides are extensively used in the microelectronics industry as interdielectric layers, passivation layers and α-particle barriers, because of their excellent chemical and physical properties[1–5]. Most aromatic polyimides are not processable due to the insolubility and high glass transition temperature ($T_g$) or high melting temperature ($T_m$), so that they are always processed in soluble precursor polymers, such as poly(amic acid)s[6–11], poly-(amic dialkyl ester)s[12–19], poly(amic silyl ester)s[20,21], and polyisoimides[22–24], and then followed by either chemical or thermal imidization.

In particular, poly(amic acid)s can be simply synthesized by low-temperature polycondensation of dianhydrides and diamines in dipolar aprotic amide solvents, such as *N,N*-dimethylformamide, *N,N*-dimethylacetamide, *N*-methyl-2-pyrrolidone, and tetramethylurea[1–11]. For this simplicity in the synthesis, poly(amic acid) precursors are widely used in the microelectronics industry. In the solution polycondensation, diamine and dianhydride reactants are weakly basic and nonprotic, respectively, and the resultant poly(amic acid) is a strong protic acid. The orthoamic acid moiety in the poly(amic acid) is a relatively strong acid because of the electron-withdrawing effect of the orthoamide group. Thus, the orthoamic acid moieties interact strongly with the dipolar aprotic amide solvent which is a Lewis base. The strong interaction is a major source of exothermicity and of driving force in the polycondensation reaction. For these reasons, the rate of poly(amic acid) formation is generally faster in more basic and more polar aprotic solvent. The synthesized poly(amic acid) is always equilibrated with the constituent monomers[10,11], and thus its molecular weight and viscosity in solution vary sensitively with temperature variation and moisture contact, causing serious problems in the quality control and fabrication process. In particular, the lack of stability of poly(amic acid)s toward hydrolysis is attributed to a catalytic effect generated by the presence of the orthocarboxylic acid moiety[19,25], in addition to the equilibration between the precursor and the constituent monomers. Thus, poly(amic acid) solutions usually need to be stored in a refrigerator before use.

Poly(amic acid) solutions are processed in several forms, such as films, coatings, fibres and powder, and followed by drying thermally or in vacuum. Then, the dried poly(amic acid)s in various forms are converted chemically or thermally to the corresponding polyimides. The chemical imidization of poly(amic acid)s is commonly performed

---

* To whom correspondence should be addressed

with the aid of acid anhydride dehydrating agents with tertiary amines via cyclodehydration[26,27]. The chemically imidized products are washed and finally dried thermally or in vacuum to remove residual solvents. On the other hand, the thermal imidization is carried out by heat-treatment up to 200–400°C, depending upon the thermal stability of the resultant polyimide[10,28–37]. In general, the imidization kinetic depends upon the backbone structure of precursor, solvent, temperature and catalyst.

In fact, the thermal imidization of poly(amic acid)s has been investigated in detail by a number of research groups[28–37], despite the nature of complexity. However, the glass transition of poly(amic acid)s has been rarely examined. There are two main difficulties in direct measurements of $T_g$ values in poly(amic acid)s with solvent free: first, poly(amic acid)s form complexes with dipolar aprotic solvents through strong interactions between the orthoamic acid groups of the precursor polymer and the basic solvent molecules, so that it is very difficult to remove all solvent molecules from cast poly(amic acid) specimens by drying. Each orthoamic acid group of poly(amic acid)s in N-methyl-2-pyrrolidone (NMP) is known to complex with one or two NMP molecules[33]. For this complex formation, dried poly(amic acid) specimens still contain typically >20 wt.% of NMP, depending on the drying conditions[31–38]. The residual solvent significantly reduces $T_g$ values of poly(amic acid)s, and furthermore, influences severely the imidization kinetic of poly(amic acid)s. Second, aromatic poly(amic acid)s exhibit relatively high $T_g$ due to their relatively high chain rigidities. Over the $T_g$ range or below, they start to imidize to the corresponding polyimides. In general, most poly(amic acid)s in dried specimens initiate to imidize about 130°C, and their imidizations are accelerated with increasing temperature[28–32]. That is, the glass transitions of most aromatic poly(amic acid)s are overlapped with or higher than their imidization temperatures. Despite these difficult circumstances, measurements of glass transition have been attempted for numerous aromatic poly(amic acid)s. However, the $T_g$ values of only a few poly(amic acid)s have been measured which were lower than 130°C, the onset temperature of imidization[34,39]. For example, poly(4,4'-oxydiphenylene 3,3',4,4'-oxydiphthalamic acid) in specimens was measured to have a $T_g$ of 125°C by differential scanning calorimetry (d.s.c.)[39]. Also, poly(4,4'-oxydiphenylene-co-p-phenylene benzophenonetetracarboxamic acid) was characterized to exhibit a $T_g$ of 125°C in dynamic mechanical thermal spectra[34]. For these poly(amic acid)s, the specimens still contained some amounts of residual solvent, so that the measured $T_g$ values are not the true glass transition temperatures.

In the present study, several poly(amic acid)s with various chain rigidities were synthesized in NMP solvent by conventional polycondensation reaction of aromatic dianhydrides and diamines: poly(p-phenylene biphenyltetracarboxamic acid), poly(p-phenylene pyromellitamic acid), and poly(4,4'-oxydiphenylene biphenyltetracarboxamic acid). The synthesized poly(amic acid) solutions were cast on glass slides and softbaked, followed by further drying in vacuum. $T_g$ values of the dried precursor samples were attempted to measure, using oscillating differential scanning calorimetry (O-d.s.c.) technique[40–45]. In addition, amounts of residual NMP solvent in the precursor samples were determined by nuclear magnetic resonance (n.m.r.) spectroscopy. The $T_g$ values of the poly(amic acid)s in solvent free were estimated from the best fitting of $T_g$ values measured with varying residual NMP content by a modified

Gordon–Taylor equation[46,47]. The true $T_g$ values estimated were interpreted with considering the chain rigidity of poly(amic acid) precursors.

## EXPERIMENTAL

### Materials and characterization

Aromatic dianhydrides and diamines used in this study were supplied by Aldrich Chemical Company and Chriskev Company: pyromellitic dianhydride (PMDA), biphenyl-tetracarboxylic dianhydride (BPDA), p-phenylene diamine (PDA), and 4,4'-oxydiphenylene diamine (ODA). All monomers were purified by sublimation under reduced pressure and then used for polymerization.

Poly(p-phenylene biphenyltetracarboxamic acid) (BPDA-PDA) was prepared in a glove box filled with dry nitrogen gas by slowly adding the sublimed BPDA to the purified PDA in dry N-methyl-2-pyrrolidone (NMP) with a boiling point of 202°C and a melting point of −23.6°C. Once the dianhydride addition was completed, the reaction flask was capped tightly and stirring was continued for 2 days to make the polymerization mixture completely homogeneous. Other poly(amic acid)s were prepared in the same manner as BPDA-PDA was synthesized: BPDA-ODA and PMDA-PDA precursors (see *Figure 1*). The solid content of the precursor solutions was 10–15 wt%. The precursor solutions were filtered with silver metal membranes of 1.0 μm pore size, tightly sealed, and stored in a refrigerator before use.

In the synthesis of poly(amic acid)s, molecular weights were attempted to be controlled by stoichiometric imbalance of the monomers using the diamine in small excess. For the synthesized poly(amic acid)s, intrinsic viscosity [η] measurements were carried out in NMP at 25.0°C using an Ubbelohde suspended level capillary viscometer, as described in the literature[48,49]. Here, in order to minimize polyelectrolyte effect in the viscosity measurement, NMP was purified by distillation over phosphorus pentoxide ($P_2O_5$) under reduced pressure and further treated with 0.02 M $P_2O_5$, followed by filtration before use[48,49]. All the solutions were filtered through 0.5 μm Fluoropore filters (Millipore) before measurement. For a given poly(amic acid), the relative and specific viscosities were measured at four different concentrations over the range of 0.10–0.60 g/dl, and the [η] value was determined by extrapolation of the reduced and inherent viscosities to infinite dilution. The [η] was determined to be 0.683 dl/g for the BPDA-PDA precursor, 0.690 dl/g for the BPDA-ODA precursor, and 0.538 dl/g for the PMDA-PDA precursor.

Poly(amic acid) solutions were cast on precleaned glass slides and softbaked on a hotplate of 80°C for 10–60 min. Some of the films softbaked for 1 h were further dried in a vacuum oven at 50°C for various times: 2, 4 and 7 days. The contents of residual NMP in these precursor films were determined by proton nuclear magnetic resonance (n.m.r.) spectroscopy as described in the following: small pieces of a dried precursor film were dissolved in dimethyl-$d_6$ sulph-oxide (DMSO-$d_6$), and the residual NMP and precursor polymer in the solution were characterized using a Bruker NMR spectrometer (Model: Aspect 300 MHz) with a proton probe. Then, the amount of NMP in weight percent was estimated from the measured n.m.r. spectra.

Glass transition and imidization temperatures of the dried precursor samples were measured in either ordinary mode or oscillating mode over −60–400°C under dry nitrogen gas flow using a Seiko oscillating differential scanning
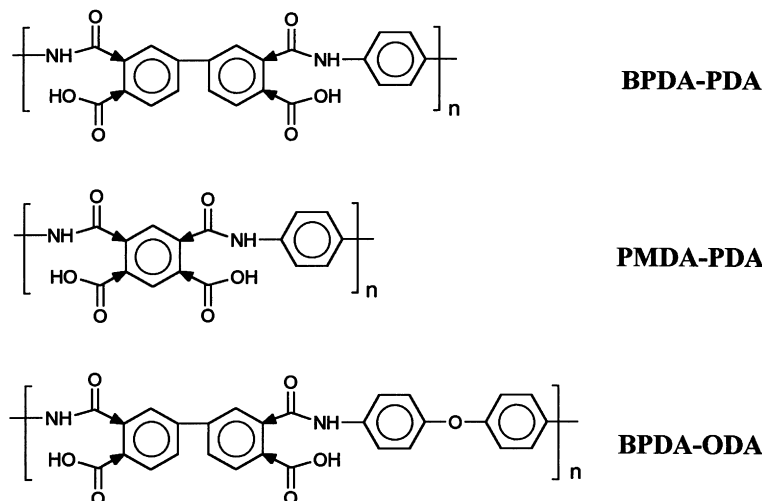
**BPDA-PDA**

**PMDA-PDA**

**BPDA-ODA**

**Figure 1**  Chemical structures of aromatic poly(amic acid)s synthesized in this study

calorimeter (Model: ODSC-220CU). During the measurements, dry nitrogen gas was purged with a flow rate of 80 cc/min. Temperature calibration was carried out using indium and tin and enthalpy calibration using indium. In the scanning run, a sample of 2 mg was used. A heating rate of 10.0 K/min was employed. An oscillating amplitude of 10.0°C and an oscillating frequency of 0.02 Hz were used, respectively.

*Oscillating differential scanning calorimetry*

The oscillating differential scanning calorimetry (O-d.s.c.) technique is briefly described here. In contrast to the ordinary differential scanning calorimetry, in which the input signal consists of only a linear component, the input signal $T(t)$ of O-d.s.c. in temperature is composed of linear and oscillating components as described in the following[40–45]:

$$T(t) = T_o + T_{ramp}(t) + T_{os}(t) \qquad (1)$$

$$= T_o + Bt - A\sin(2\pi ft) \qquad (2)$$

where $T_o$, $T_{ramp}$ $(=Bt)$ and $T_{os}$ $[= -A\sin(2\pi ft)]$ are the start temperature, the linear heating component, and the oscillating heating component, respectively. $A$ and $B$ are the oscillating amplitude and the heating rate, respectively, whereas $t$ and $f$ are the time and the oscillating frequency, respectively. For the O-d.s.c. used in this study, the oscillating frequency $f$ is in the range of 0.01–0.1 Hz.

The output signal in the O-d.s.c. is also composed of linear and oscillating components. Thus, the output signal $Y(t)$ (namely, total heat flow) can be separated into two signal components in the following:

$$Y(t) = Y_{ramp}(t) + Y_{os}(t) \qquad (3)$$

where $Y_{ramp}(t)$ and $Y_{os}(t)$ are the linear and the oscillating d.s.c. signal components, respectively. In addition, the total heat flow can be also expressed by the sum of the specific heat flow $Y_{sp}(t)$ and the kinetic heat flow $Y_k(t)$. Thus, equation (3) can be rewritten below:

$$Y(t) = Y_{sp}(t) + Y_k(t). \qquad (4)$$

Here, the specific heat flow appears in thermally reversible phenomena such as glass transition and melting transition. On the other hand, the kinetic heat flow appears in thermally irreversible phenomena such as chemical reaction, evaporation, and decomposition.

The specific heat flow component $Y_{sp}(t)$ in equation (4) can be expressed by a function of the temperature $T(t)$ of equation (1) and the heat capacity $C_p$, whereas the oscillating d.s.c. signal component $Y_{os}(t)$ in equation (3) can be described by a function of the oscillating temperature $T_{os}(t)$ in equation (1) and $C_p$:

$$Y_{sp}(t) = -C_p \frac{dT(t)}{dt} \qquad (5)$$

and

$$Y_{os}(t) = C_p \frac{dT_{os}(t)}{dt}. \qquad (6)$$

Taking into account equation (2) and equation (6), $Y_{sp}(t)$ in equation (5) can be obtained as the following form:

$$Y_{sp}(t) = \left[\frac{B}{2\pi f} - A\cos(2\pi ft)\right]\left[\frac{Y_{os}(t)}{A\cos(2\pi ft)}\right]. \qquad (7)$$

Here,

$$A\cos(2\pi ft) = A\sin\left\{2\pi f\left(t - \frac{1}{4f}\right)\right\} \qquad (8)$$

$$= T_{os}\left(t - \frac{1}{4f}\right). \qquad (9)$$

By taking into account equation (9), the specific heat flow component $Y_{sp}(t)$ is finally expressed below:

$$Y_{sp}(t) = \left[\frac{B}{2\pi f} - T_{os}\left(t - \frac{1}{4f}\right)\right]\left[\frac{Y_{os}(t)}{T_{os}\left(t - \frac{1}{4f}\right)}\right]. \qquad (10)$$

Thus, the kinetic heat flow component $Y_k(t)$ can be obtained by subtracting the specific heat flow component $Y_{sp}(t)$ from the total heat flow $Y(t)$:

$$Y_k(t) = Y(t) - Y_{sp}(t). \qquad (11)$$

As described above, the O-d.s.c. technique has several advantages, compared to the ordinary d.s.c.. The first advantage is the effective separation of specific heat flow, that appears in thermally reversible phenomena such as glass and melting transitions, from the kinetic heat flow that reveals in thermally irreversible phenomena such as chemical reaction, evaporation, and decomposition. The second is
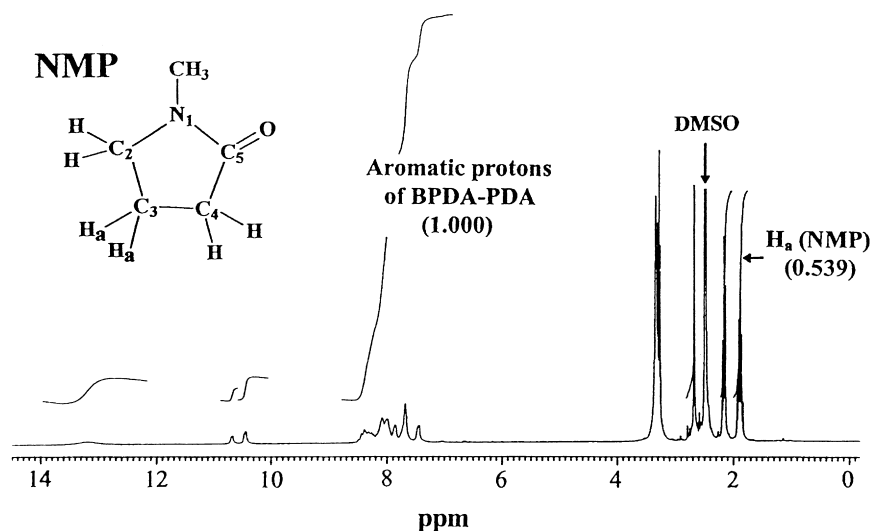
**Figure 2** $^{1}$H n.m.r. spectrum of a BPDA-PDA precursor sample softbaked at 80°C for 1 h, which was dissolved in dimethyl-$d_6$ sulphoxide (DMSO-$d_6$)

**Table 1** Compositions, glass transition (or melting) temperatures ($T_g$ or $T_m$ values), and imidization temperatures ($T_i$ values) of BPDA-PDA precursor samples dried under various conditions

| Precursor sample | Drying condition | Composition[a] | | $T_g$ (or $T_m$) (°C) | $T_i^{b}$ (°C) |
| --- | --- | --- | --- | --- | --- |
| | | NMP (wt.%) | Precursor (wt.%) | | |
| Sample #1 | (NMP itself) | 100 | 0 | $-23.6^{c}$ | — |
| #2 | (Precursor solution itself) | 88.3 | 11.7 | $-29.5^{c}$ | — |
| #3 | 80°C/10 min | 78.1 | 21.9 | $-29.2^{c}$ | — |
| #4 | 80°C/20 min | 66.4 | 33.6 | $-33.6^{c}$ | — |
| #5 | 80°C/1 h | 39.9 | 60.1 | $39.3^{d}$ | 138.7 |
| #6 | 80°C/1 h + 50°C/2 day (in vacuum) | 34.6 | 65.4 | $85.5^{d}$ | 139.0 |
| #7 | 80°C/1 h + 50°C/4 day (in vacuum) | 30.5 | 69.5 | $117.2^{d}$ | 146.9 |
| #8 | 80°C/1 h + 50°C/7 day (in vacuum) | 26.5 | 73.5 | $133.0^{d}$ | 154.7 |

[a] Measured by proton n.m.r. spectroscopy
[b] Onset temperature of imidization measured by O-d.s.c.
[c] $T_m$ measured from the peak maximum of NMP melting in ordinary differential scanning calorimetry (d.s.c.) run
[d] $T_g$ measured from the onset of glass transition in oscillating differential scanning calorimetry (O-d.s.c.) run

the precise measurement of very weak glass transition. The other is the precise measurement of specific heat changes ($\Delta C_p$ values) in glass and melting transitions.

## RESULTS AND DISCUSSION

### N.m.r. spectroscopic determination of residual solvent

In general, the glass transition of a polymer in films prepared by solution casting and subsequent drying is strongly dependent upon the amount of residual solvent. As mentioned above, poly(amic acid)s, which were synthesized in NMP solvent, form complexes with NMP molecules via strong interaction between the orthocarboxylic acid group of the precursor and the tertiary amino group of the NMP, so that NMP solvent could not be removed completely from the cast samples by drying process. The residual NMP solvent affects severely the glass transition of poly(amic acid)s. Therefore, in this study the amounts of residual NMP solvent in precursor samples dried at various conditions were measured by proton n.m.r. spectroscopy and correlated to the $T_g$ values determined independently by O-d.s.c. technique.

For a BPDA-PDA poly(amic acid) sample softbaked at 80°C for 1 h, its tiny pieces were dissolved in DMSO-$d_6$ and characterized by proton n.m.r. spectroscopy. The measured

n.m.r. spectrum is illustrated in *Figure 2*. The two protons (2Ha) of the carbon-3 ($C_3$) in the five-membered ring of NMP appeared at $\delta = 1.75$–$2.05$ ppm, whereas the 10 aromatic protons in the repeat unit of BPDA-PDA poly(amic acid) showed at $\delta = 7.3$–$8.6$ ppm as multiple peaks. The amount of NMP solvent in weight fraction ($W_s$) was estimated from the integrations of these peaks in the following:

$$W_s = \frac{\left[\dfrac{A_{2Ha}}{N_{2Ha}}\right][M_{NMP}]}{\left[\dfrac{A_{2Ha}}{N_{2Ha}}\right][M_{NMP}] + \left[\dfrac{A_{ar}}{N_{ar}}\right][M_p]} \qquad (12)$$

where $A_{2Ha}$, $N_{2Ha}$, and $M_{NMP}$ are the integration of the two proton signals, the number of $H_a$ protons, and the molecular weight of NMP, respectively, and $A_{ar}$, $N_{ar}$, and $M_p$ are the total integration of the aromatic proton signals, the number of the aromatic protons in a chemical repeat unit, and the molecular weight of the chemical repeat unit in the precursor, respectively. The NMP content in the dried film was determined to be 39.9 wt.%. Thus, the content of the precursor polymer (that is, $W_p$ in percentage) was 60.1 wt.%. For precursor samples dried at the other conditions, NMP and polymer contents were determined in the same manner.

**Table 2** Compositions, glass transition temperatures ($T_g$ values), and imidization temperatures ($T_i$ values) of PMDA-PDA precursor samples dried under various conditions

| Precursor sample | Drying condition | Composition[a] | | $T_g^b$ (°C) | $T_i^c$ (°C) |
| --- | --- | --- | --- | --- | --- |
| | | NMP (wt.%) | Precursor (wt.%) | | |
| Sample #1 | 80°C/1 h | 52.9 | 47.1 | 26.2 | 123.0 |
| #2 | 80°C/1 h + 50°C/ 2 day (in vacuum) | 44.9 | 55.1 | 88.2 | 125.4 |
| #3 | 80°C/1 h + 50°C/ 4 day (in vacuum) | 42.7 | 57.3 | 108.6 | 128.9 |
| #4 | 80°C/1 h + 50°C/ 7 day (in vacuum) | 39.6 | 60.4 | 112.8 | 131.5 |

[a]Measured by proton n.m.r. spectroscopy
[b]$T_g$ measured from the onset of glass transition in oscillating differential scanning calorimetry (O-d.s.c.)
[c]Onset temperature of imidization measured by O-d.s.c.

**Table 3** Compositions, glass transition temperatures ($T_g$ values), and imidization temperatures ($T_i$ values) of BPDA-ODA precursor samples dried under various conditions

| Precursor sample | Drying condition | Composition[a] | | $T_g^b$ (°C) | $T_i^c$ (°C) |
| --- | --- | --- | --- | --- | --- |
| | | NMP (wt.%) | Precursor (wt.%) | | |
| Sample #1 | 80°C/1 h | 41.6 | 58.4 | 31.2 | 131.3 |
| #2 | 80°C/1 h + 50°C/ 2 day (in vacuum) | 30.0 | 70.0 | 102.0 | 136.1 |
| #3 | 80°C/1 h + 50°C/ 4 day (in vacuum) | 26.2 | 73.8 | 113.8 | 140.3 |
| #4 | 80°C/1 h + 50°C/ 7 day (in vacuum) | 25.8 | 74.2 | 115.1 | 149.3 |

[a]Measured by proton n.m.r. spectroscopy
[b]$T_g$ measured from the onset of glass transition in oscillating differential scanning calorimetry (O-d.s.c.)
[c]Onset temperature of imidization measured by O-d.s.c.
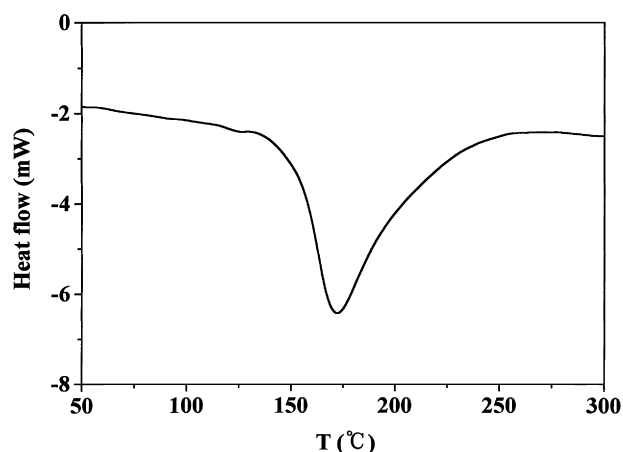


**Figure 3** The ordinary d.s.c. thermogram of a BPDA-PDA precursor sample containing 26.5 wt.% residual NMP solvent. A heating rate of 10.0 K/min was employed

As summarized in *Table 1*, the precursor solution contained 88.3 wt.% NMP, and the dried precursor samples had 26.5–78.1 wt.% NMP, depending on the drying conditions.

Similar characterization of residual NMP was performed for PMDA-PDA and BPDA-ODA precursor samples dried at various conditions. The results are listed in *Tables 2* and *3*, respectively. For PMDA-PDA precursor, the sample dried at 80°C/1 h contained 52.9 wt.% NMP, and the other samples had 39.6–44.9 wt.% NMP, depending on the drying conditions. For BPDA-ODA precursor, the sample

dried at 80°C/1 h contained 41.6 wt.% NMP, and the other samples had 25.8–30.0 wt.% NMP, depending on the drying conditions.

Overall, the content of residual NMP in the dried precursor sample was dependent first on the initial concentration of the precursor solution and then reduced by drying: longer drying time gave lower residual NMP. The lowest NMP content was 26.5 wt.% for the BPDA-PDA precursor sample, 39.6 wt.% for the PMDA-PDA precursor, and 25.8 wt.% for the BPDA-ODA precursor: here, all the precursor samples were dried for 7 days at 50°C in vacuum. For these highly dried precursor samples, all the residual NMP molecules are assumed to participate in forming complexes with the orthoamic acid groups of the precursors and then the number of NMP molecules bound to the repeat units of the precursors can be estimated from the contents of residual NMP measured by n.m.r. spectroscopy. The number of the NMP molecules bound per chemical repeat unit of precursor is calculated to be 1.4 for the BPDA-PDA, 2.1 for the PMDA-PDA, and 1.7 for the BPDA-ODA precursor. These are in good agreement with the results published previously in the literature[33].

*O-d.s.c. measurements*

A BPDA-PDA precursor sample with a residual NMP of 26.5 wt.% was characterized by ordinary and oscillating d.s.c. techniques. From the ordinary d.s.c. thermogram in *Figure 3*, the heat flow curve of glass transition is not recognizable because the endothermic heat flow due to the imidization is very dominant over the temperature range of 115–280°C. Thus, only the imidization temperature of the precursor sample can be estimated from the ordinary d.s.c. thermogram. In contrast, *Figure 4* shows the oscillating input temperature signals as well as the oscillating d.s.c. output signals as a function of time. The O-d.s.c. thermogram can be nicely separated into two parts, the specific heat flow and the kinetic heat flow, by equation (10) and equation (11) described in the Experimental Section. The separated specific and kinetic heat flows are plotted in *Figure 5* as a function of temperature. The specific heat flow curve reveals clearly glass transition over 115–165°C. From this thermogram, $T_g$ was determined to be 133.0°C for the dried precursor sample: here, $T_g$ is defined as the onset temperature of glass transition in the specific heat flow. On the other hand, the kinetic heat signal curve shows a broad, big endothermic heat flow peak which results from the imidization reaction and the removal of the reaction byproduct (i.e. water) and residual solvent. The onset temperature of imidization ($T_i$) in the dried film was estimated to be 148.1°C.

The O-d.s.c. measurement was carried out for the other BPDA-PDA precursor samples dried at various conditions. For the precursor samples with a residual NMP of <50 wt.%, the separated specific heat and kinetic heat flow curves are illustrated in *Figures 6* and *7*, respectively, and compared with those of the sample described above, respectively. Both $T_g$ and $T_i$ of each sample were estimated from the heat flow curves and listed in *Table 1*. As the content of residual NMP in the precursor sample reduced to 26.5 wt.% from 39.9 wt.%, $T_g$ increased to 133.0 from 39.3°C and $T_i$ also increased to 154.7°C from 138.7°C. Overall, the residual NMP in the precursor sample caused the lowering of both glass transition and imidization temperatures. However, the effect of residual NMP is relatively much higher in the $T_g$ than the $T_i$.

The O-d.s.c. investigation was extended to the precursor
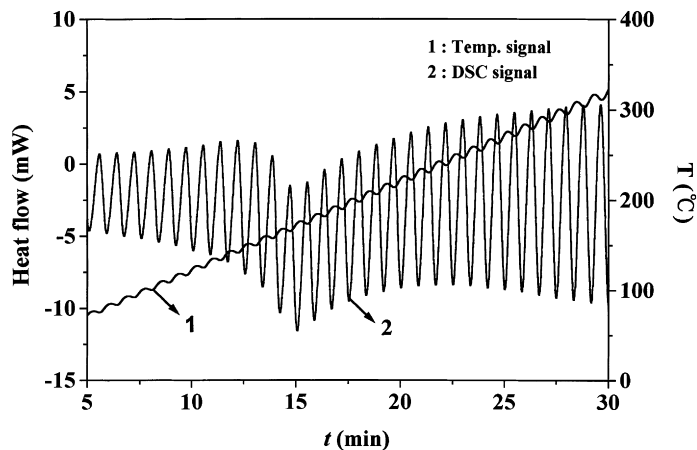
**Figure 4** The input temperature signal and out O-d.s.c. signal of a BPDA-PDA precursor sample containing 26.5 wt.% residual NMP solvent. A heating rate of 10.0 K/min was employed. The temperature amplitude and frequency used in the oscillation were 10.0°C and 0.02 Hz, respectively

samples which contained >50 wt.% NMP, including NMP itself as well as the precursor solution itself, with a concentration of 11.7 wt.%. These samples exhibited glass transition or melting transition at a temperature region much lower than their imidization temperature, so that measurements were carried out in the ordinary mode. The results are listed in *Table 1*. The melting point ($T_m$) of the pure NMP was −23.6°C: Here, $T_m$ is defined as the temperature of the peak maximum of NMP melting in the ordinary d.s.c. signal. For the precursor samples, including the precursor solution, the $T_m$ of NMP component was depressed, depending on the content of precursor polymer. $T_m$ was measured to be −29.5°C for the precursor solution itself with 11.7 wt.% precursor, −29.2°C for the sample with 21.9 wt.% precursor, and −33.6°C for the sample with 33.6 wt.% precursor.

In addition, from these $T_g$ (or $T_m$) data with varying compositions, it has been attempted to make a phase diagram for the BPDA-PDA precursor/NMP mixture. The measured $T_g$ values (or $T_m$ values) are plotted in *Figure 8*. The $T_m$ in the mixture with the major NMP component decreases linearly with increasing precursor content, whereas the $T_g$ in the mixture with the major precursor component decreases convexly with increasing NMP content. They are extrapolated to meet at a composition of 49.2 wt.% NMP and 50.8 wt.% precursor. In particular, the solid curve line at a concentration of >50.8 wt.% precursor is a curve fitted by a modified Gordon–Taylor equation. This will be described in detail below.

Both PMDA-PDA and BPDA-ODA precursors in the dried sample were characterized by O-d.s.c. in the same manner as the BPDA-PDA precursor samples were investigated. For all the O-d.s.c. thermograms, the specific heat flow parts were separated from the kinetic heat flow parts. Both $T_g$ and $T_i$ values, which were estimated from the separated specific and kinetic heat flow curves, respectively, are summarized in *Tables 2* and *3*. For PMDA-PDA samples, as the content of residual NMP varied from 52.9 to 39.6 wt.%, $T_g$ increased from 26.2 to 112.8°C, whereas $T_i$ also increased from 123.0 to 131.5°C. Similar dependency of residual NMP in both $T_g$ and $T_i$ was observed for the BPDA-ODA precursor sample. $T_g$ in the precursor sample varied in the range of 31.2–115.1°C and $T_i$ varied over the range of 131.3–149.3°C, depending on the content of NMP. Overall, for the precursor samples, higher NMP
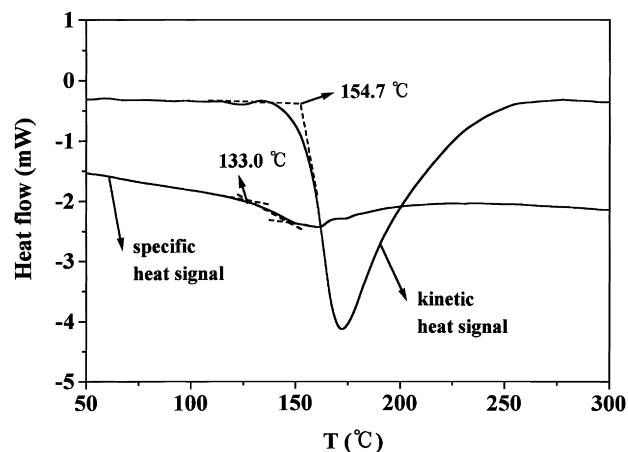


**Figure 5** The signals of specific and kinetic heat flow component separated from the O-d.s.c. thermogram in *Figure 4*, which was obtained for a BPDA-PDA precursor sample containing 26.5 wt.% residual NMP solvent
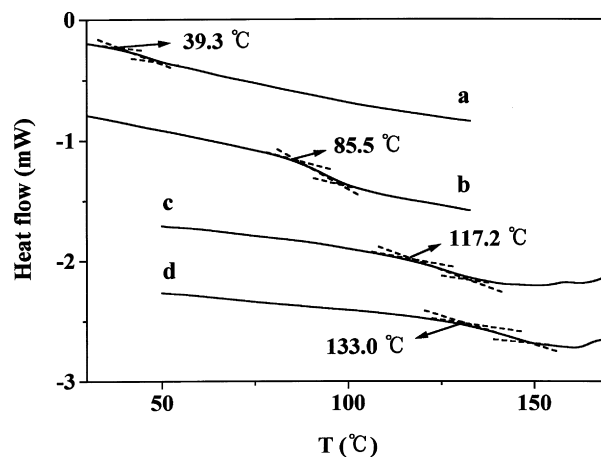


**Figure 6** The signals of specific heat flow component separated from O-d.s.c. thermograms obtained for BPDA-PDA precursor samples containing various amounts of residual NMP: (a) 39.9 wt.% NMP; (b) 34.6 wt.%; (c) 30.5 wt.%; (d) 26.5 wt.%. A heating rate of 10.0 K/min was employed. The temperature amplitude and frequency used in the oscillation were 10.0°C and 0.02 Hz, respectively

content caused lower $T_g$ and $T_i$, as observed in the BPDA-PDA precursor sample.

### Estimation of $T_g$ values of poly(amic acid) precursors with solvent free

From the $T_g$ values measured from the precursor samples contained residual NMP, it was attempted in this section to estimate true $T_g$ values of the poly(amic acid) precursors, namely, $T_g$ values of the precursors in solvent free. This is possible by a reasonable theoretical analysis of the measured $T_g$ values.

$T_g$ *versus* composition in miscible binary blends of polymers and plasticizers was reported to have many variations[46–57]. For polymer blends miscible over the entire range of composition, three generalized $T_g$-composition curves are reported: (i) the linear relationship[50,51]; (ii) the concave deviation from the linearity[52–54]; and (iii) the convex deviation from the linearity[55–57]. Both the linear and concave relationships indicate the miscibility results
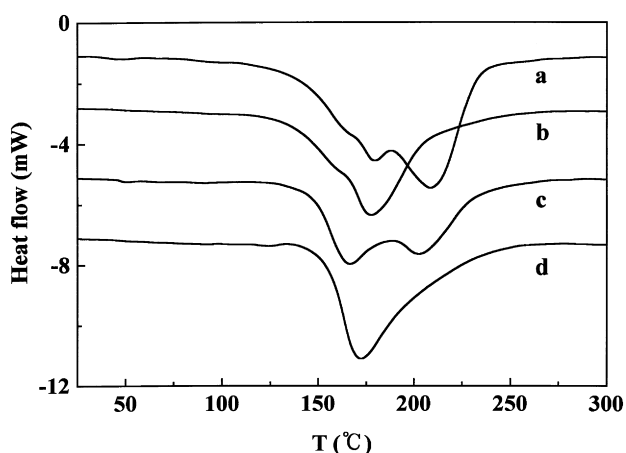
**Figure 7** The signals of kinetic heat flow component separated from O-d.s.c. thermograms obtained for BPDA-PDA precursor samples containing various amounts of residual NMP: (*a*) 39.9 wt.% NMP; (b) 34.6 wt.%; (c) 30.5 wt.%; (d) 26.5 wt.%. A heating rate of 10.0 K/min was employed. The temperature amplitude and frequency used in the oscillation were 10.0°C and 0.02 Hz, respectively
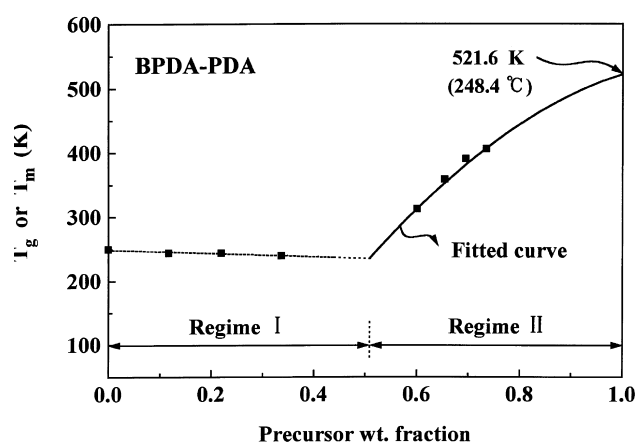
**Figure 8** The variation of glass transition temperature ($T_g$) or melting point ($T_m$) of BPDA-PDA precursor/NMP mixture as a function of precursor weight fraction. The ■ symbols denote the measured phase transition temperatures. The solid curve is the curve fitted by a modified Gorden–Taylor equation, equation (18) from the $T_g$ data measured in the *regime* II

from the intermolecular interaction based on mainly van der Waals attraction between the blend components. On the other hand, the convex relationship is known to result from strong intermolecular interactions, such as hydrogen bonding, acid–base interaction, and charge complexation, between the blend components. These $T_g$ variations with composition were attempted to be described by several theoretical and empirical expressions, such as the Fox[52], Gordon–Taylor[53], Kelley–Bueche[54], Gibbs–Dimarzio[58], Kanig[59], Wood[60], modified Fox[61], modified Gibbs–Dimarzio[62], and modified Gordon–Taylor[46,47], equations: here, it is noted that some of these equations have been originally developed to illustrate $T_g$ variations in copolymers.

In particular, convex $T_g$ behaviours with composition observed in miscible polymer–polymer blend systems with strong interactions between the components[56,57] have been successfully described by a modified Gordon–Taylor equation, that was introduced for copolymer systems by Jenckel *et al.*[46] and Uemastu *et al.*[47] For example, the convex $T_g$ behaviour in the blend of poly(vinyl nitrate) and poly(vinyl acetate) obeyed the modified Gordon–Taylor expression[57]. The modified Gordon–Taylor expression was adapted in the present study in order to illustrate convex $T_g$ variations with composition in the poly(amic acid)s contained residual NMP solvent via strong acid–base complexation between the orthoamic acid group of the polymers and the secondary amino group of the NMP molecules and, furthermore, to estimate their true $T_g$ values in residual solvent free.

The modified Gordon–Taylor equation can be expressed in the following[46–57]:

$$T_g = \frac{\Delta\alpha_s T_{g,s} W_s + \Delta\alpha_p T_{g,p} W_p}{\Delta\alpha_s W_s + \Delta\alpha_p W_p} + \frac{\Delta k W_s W_p}{\Delta\alpha_s W_s + \Delta\alpha_p W_p} \quad (13)$$

where

$$\Delta\alpha_i = \alpha_{r,i} - \alpha_{g,i} \quad (14)$$

and

$$\Delta k = k_g - k_r. \quad (15)$$

Here, $T_g$ is the glass transition temperature of a mixture containing the weight fractions, $W_s$ and $W_p$, of two components (i.e. NMP solvent, s and precursor polymer, p) in which glass transition temperatures are $T_{g,s}$ (that is, melting point ($T_m$) of NMP) and $T_{g,p}$, respectively. $\Delta\alpha_i$ is the difference between the volume expansion coefficients, $\alpha_{r,i}$ and $\alpha_{g,i}$, of the component $i$ in the rubbery (or liquid) and glassy states. $k_g$ and $k_r$ are the parameters representing the volume changes on mixing of two components in a mixture as expressed in the following:

$$V_g = V_{g,s} W_s + V_{g,p} W_p + k_g W_s W_p \quad (16)$$

and

$$V_r = V_{r,s} W_s + V_{r,p} W_p + k_r W_s W_p \quad (17)$$

where $V_g$ and $V_r$ are the specific volumes of a mixture in the glassy and rubbery (or liquid) states, respectively. $V_{g,i}$ and $V_{r,i}$ are the specific volumes of the component $i$ in the glassy and rubbery (or liquid) states, respectively. The changes in the specific volumes with the temperature are assumed to be linear.

In this study, poly(amic acid) precursors contained residual NMP solvent were observed to exhibit a *two-regime* behaviour in the phase transition with composition. For the BPDA-PDA precursor/NMP mixture shown in *Figure 8*, in

**Table 4** Constants used in estimating the $\Delta k$ of BPDA-PDA poly(amic acid)

| Constant | |
|---|---|
| $\Delta\alpha_s$ | $3.27 \times 10^{-4}$ cc/g·K |
| $\Delta\alpha_p$ | $2.69 \times 10^{-4}$ cc/g·K |
| $\Delta\alpha_1$ | $2.92 \times 10^{-4}$ cc/g·K |
| $\Delta\alpha_3$ | $2.84 \times 10^{-4}$ cc/g·K |
| $\Delta T_2$ | 9.6 K |
| $\Delta T_{2'}$ | 12.4 K |
| $W_3 - W_1$ | 0.143 |

**Table 5** Constants used to estimate $T_g$ values of poly(amic acid)s in solvent free[a]

| Precursor | $V_w$ (cc/g) | $\Delta\alpha$ (cc/g·K) | $\Delta k$ | $W_c$ | $T_g$ (°C) |
|---|---|---|---|---|---|
| BPDA-PDA | 0.488 | $2.69 \times 10^{-4}$ | $0.106 \times (1 - W_c)$ | 0.521 | 248.4 |
| PMDA-PDA | 0.507 | $2.79 \times 10^{-4}$ | $0.106 \times (1 - W_c)$ | 0.404 | 283.4 |
| BPDA-ODA | 0.497 | $2.74 \times 10^{-4}$ | $0.106 \times (1 - W_c)$ | 0.505 | 184.4 |

[a] The $V_w$ and $\Delta\alpha$ of the pure NMP solvent were calculated to be 0.595 cc/g and $3.27 \times 10^{-4}$ cc/g·K, respectively
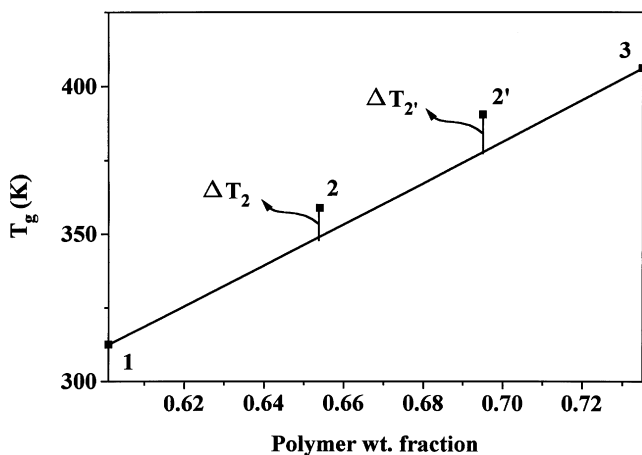
**Figure 9** The variation of glass transition temperature ($T_g$) of BPDA-PDA precursor/NMP mixture in the *regime* II as a function of precursor weight fraction: The ■ symbols, which are denoted by 1, 2, 2′, and 3, are the $T_g$ values measured by O-d.s.c. The solid line is the line fitted by the simple Gorden–Taylor equation, equation (21) from the measured $T_g$ data. $\Delta T_2$ is the difference between the measured and calculated $T_g$ for the sample containing 34.6 wt.% NMP, whereas $\Delta T_{2'}$ is the difference for the sample containing 30.5 wt.% NMP
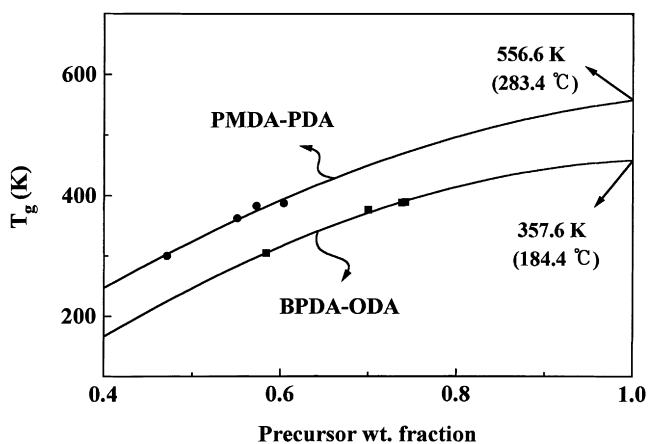
**Figure 10** Variations of glass transition temperatures ($T_g$ values) of PMDA-PDA precursor/NMP mixture and BPDA-ODA precursor/NMP mixture as a function of precursor weight fraction. The ■ symbols denote the measured phase transition temperatures. The solid curves are the curves fitted by a modified Gorden–Taylor equation, equation (18) from measured $T_g$ data

the solvent-rich region (that is, *regime* I) $T_g$ decreases linearly with increasing the precursor concentration until reaching to a critical concentration ($W_c$), which is perhaps related to the gel point, because the melting point (or freezing point) depression of NMP due to the dissolution of the poly(amic acid) with a high molecular weight. After reached to a critical concentration ($W_c$), the mixture gets into the precursor rich region (i.e. *regime* II), and $T_g$ is inverted to increase with further increasing the precursor concentration. Consequently, for only the *regime* II, $T_g$ increases convexly with varying composition. Thus, the modified Gorden–Taylor equation, equation (13) cannot be directly applicable for the entire compositions in the mixture of a poly(amic acid) and NMP solvent. That is, equation (13) can be applicable to the mixtures in only the *regime* II.

For the application of equation (14) to the precursor/NMP mixtures limited in the *regime* II, it was further modified in the following. In equation (13) the $\Delta\alpha_s$ and $T_{g,s}$ terms of the pure solvent are replaced by the $\Delta\alpha_c$ and $T_{g,c}$ terms of the mixture with the critical concentration $W_c$ and the weight fractions ($W_s$ and $W_p$) of solvent and precursor in a mixture are again fractionated by the $(1 - W_c)$ term rather than 1.0, which covers the entire concentration range, respectively:

$$T_g = \frac{\Delta\alpha_c T_{g,c}\left(\dfrac{1 - W_p}{1 - W_c}\right) + \Delta\alpha_p T_{g,p}\left(\dfrac{W_p - W_c}{1 - W_c}\right)}{\Delta\alpha_c\left(\dfrac{1 - W_p}{1 - W_c}\right) + \Delta\alpha_p\left(\dfrac{W_p - W_c}{1 - W_c}\right)}$$
$$+ \frac{\Delta k\left(\dfrac{1 - W_p}{1 - W_c}\right)\left(\dfrac{W_p - W_c}{1 - W_c}\right)}{\Delta\alpha_c\left(\dfrac{1 - W_p}{1 - W_c}\right) + \Delta\alpha_p\left(\dfrac{W_p - W_c}{1 - W_c}\right)} \quad (18)$$

where

$$W_c \leq W_p \leq 1.0 \quad (19)$$

and

$$\Delta\alpha_c = \Delta\alpha_s(1 - W_c) + \Delta\alpha_p W_c. \quad (20)$$

$\Delta\alpha_s$ and $\Delta\alpha_p$ were calculated from the van der Waals volumes ($V_w$ values)[63,64] of the repeating unit of a precursor and the NMP solvent molecule, respectively, as described previously in the literature[65]. The results are summarized in *Tables 4* and *5*.

In addition, for a given precursor/NMP system, $\Delta k$ ($= k_g - k_r$) cannot be obtained conveniently. Thus, an estimate of $\Delta k$ was attempted by analysing the $T_g$ data measured for a precursor/NMP mixture with various compositions in the following manner. For the BPDA-PDA precursor/NMP mixture, four $T_g$ data points in the *regime* II are plotted in *Figure 9* as a function of the weight fraction of the precursor, and fitted by the simple Gordon–Taylor equation[62], as shown below, using the lowest and highest $T_g$ data points (namely, points 1 and 3 in *Figure 9*) as the reference $T_g$ values:

$$T_g = \frac{\Delta\alpha_s T_{g,s} W_s + \Delta\alpha_p T_{g,p} W_p}{\Delta\alpha_s W_s + \Delta\alpha_p W_p}. \quad (21)$$

In *Figure 9*, the two $T_g$ points (that is, $T_{g,2}$ and $T_{g,2'}$) in the

intermediate region can be calculated by the following equations, respectively:

$$T_{g,2} = \frac{\Delta\alpha_1 T_{g,1}(W_3 - W_2) + \Delta\alpha_3 T_{g,3}(W_2 - W_1)}{\Delta\alpha_1(W_3 - W_2) + \Delta\alpha_3(W_2 - W_1)} \quad (22)$$

and

$$T_{g,2'} = \frac{\Delta\alpha_1 T_{g,1}(W_3 - W_{2'}) + \Delta\alpha_3 T_{g,3}(W_{2'} - W_1)}{\Delta\alpha_1(W_3 - W_{2'}) + \Delta\alpha_3(W_{2'} - W_1)} \quad (23)$$

where 1, 2, 2′, and 3 denote the mixtures with four different weight fractions ($W_1$, $W_2$, $W_{2'}$, and $W_3$) of the precursor, respectively. Here, $\Delta\alpha_1$ and $\Delta\alpha_3$ are expressed below:

$$\Delta\alpha_1 = \Delta\alpha_s(1 - W_1) + \Delta\alpha_p W_1 \quad (24)$$

and

$$\Delta\alpha_3 = \Delta\alpha_s(1 - W_3) + \Delta\alpha_p W_3. \quad (25)$$

However, the measured $T_{g,2}$ and $T_{g,2'}$ are deviated by $\Delta T_2$ and $\Delta T_{2'}$ from the $T_g$ values calculated by equation (22) and equation (23), respectively, as shown in *Figure 9*. These deviations can be expressed by an equation in the following, as previously described for the modified Gordon–Taylor equation:

$$\Delta T_2 = \frac{\Delta k_2'(W_3 - W_2)(W_2 - W_1)}{\Delta\alpha_1(W_3 - W_2) + \Delta\alpha_3(W_2 - W_1)} \quad (26)$$

and

$$\Delta T_{2'} = \frac{\Delta k_{2'}'(W_3 - W_{2'})(W_{2'} - W_1)}{\Delta\alpha_1(W_3 - W_{2'}) + \Delta\alpha_3(W_{2'} - W_1)}. \quad (27)$$

From these equations, $\Delta k_2'$ and $\Delta k_{2'}'$ were calculated to be 0.012 and 0.017, respectively. The calculated $\Delta k_2'$ and $\Delta k_{2'}'$ were averaged to give $\Delta k'$:

$$\Delta k' = \frac{\Delta k_2' + \Delta k_{2'}'}{2} \quad (28)$$

The calculated $\Delta k_2'$ and $\Delta k_{2'}'$ exhibit slightly different values, indicating that $\Delta k'$ is a function of the mixture composition. Thus, the $\Delta k'$ is normalized over the composition range (that is, $(W_3 - W_1)$) considered, and then further generalized for the *regime* II by multiplying $(1 - W_c)$, giving $\Delta k$:

$$\Delta k = \Delta k' \left( \frac{1 - W_c}{W_3 - W_1} \right) \quad (29)$$

$$= 0.106(1 - W_c). \quad (30)$$

Consequently, $\Delta k$ is expressed as a function of the critical concentration ($W_c$). The parameters used in the estimation of $\Delta k$ are listed in *Table 4*.

With the estimated $\Delta k$, $T_g$ data measured for the BPDA-PDA precursor mixtures in the *regime* II were tried to be fitted by equation (18) with varying $W_c$. As shown in *Figure 8*, the best fitted result was obtained with $W_c = 0.521$, resulting in $T_g = 248.4°C$ for the BPDA-PDA precursor in solvent free.

The $\Delta k$ estimated for the BPDA-PDA precursor mixture was used to analyse of $T_g$ data of the other precursor mixtures without further modification. For the PMDA-PDA precursor mixture, $T_g$ values measured over the *regime* II were fitted by equation (18). The $W_c = 0.404$ gave the best result in the fitting (see *Figure 10*). The $T_g$ of PMDA-PDA precursor without solvent was estimated to be

283.4°C. $T_g$ values of the BPDA-ODA precursor mixtures were best fitted by equation (18) with $W_c = 0.505$, giving $T_g = 184.4°C$ for the precursor in solvent free (see *Figure 10*). The $T_g$ values of the precursors in solvent free are listed with the constants used for their estimations in *Table 5*.

*Chain rigidities and their relationship to $T_g$ values in poly(amic acid)s*

In general, the chain rigidity of a polymer, which is known to play a critical role in the glass transition, is characterized by the statistical segment proposed by Kuhn[66], so-called Kuhn statistical segment. The Kuhn statistical segment ($L_K$) in a polymer chain is defined below:

$$L_K = \frac{\langle h^2 \rangle}{l} \quad (31)$$

$$= \frac{1}{\lambda} \frac{\langle h^2 \rangle}{n} \quad (32)$$

where $\langle h^2 \rangle$, $l$, and $n$ are the mean square of end-to-end distance, the contour length (that is, the length of a fully extended chain), and the number of structural repeat units in a precursor polymer. $\lambda$ is defined by $l/n$. Here, the mean square of end-to-end distance per a structural repeat unit, $\langle h^2 \rangle/n$ can be estimated by a method described by Birshtein and co-workers[67,68]:

$$\frac{\langle h^2 \rangle}{n} = \sum_{\alpha=1}^{v} \sum_{\delta=0}^{v-1} \left[ \frac{l_\alpha l_{[\alpha+\delta]}\{(\cos\gamma)^\delta + (\cos\gamma)^{v-\delta}\}}{1 - (\cos\gamma)^v} \right] \quad (33)$$

with

$$[\alpha + \delta] : \alpha + \delta \quad \text{for } (\alpha + \delta) \le v \quad \text{or}$$

$$\alpha + \delta - v \quad \text{for } (\alpha + \delta) > v. \quad (34)$$

Here, $v$, $l_\alpha$, and $(\pi - \gamma)$ are the number of linear bonds in a structural repeating unit, the length of the $\alpha$th bond, and the angle between the links, respectively.

Using equation (32) and equation (33) the Kuhn statistical segments of the precursor polymers considered were calculated in this study. The calculations were carried out with three assumptions in the following. First, the amide linkage in the repeat unit of a poly(amic acid) possesses a planar *trans*-structure[69]. Second, in the poly(amic acid)s all the backbone skeletal valence angles, such as $\angle C_{ar}-C-N$, $\angle C-N-C_{ar}$, and $\angle C_{ar}-O-C_{ar}$ (see *Figure 11*), are equal to be 120°, as adapted previously by Birshtein *et al.*[67] in their calculations for polyimides. Finally, the precursors are alternatively linked by possible isomeric repeat units. For both BPDA-PDA and BPDA-ODA precursors, the chemical repeat units have four different isomeric structures as shown in *Figure 11*: *meta–para*, *meta–meta*, *para–para*, and *para–meta* isomers. The chemical repeat unit of PMDA-PDA precursor has two isomeric structures: *meta* and *para* isomers (see *Figure 11*).

The calculated results are listed in *Table 6* with $T_g$ values determined in the previous section. The calculated Kuhn statistical segment was 62.2 Å for the BPDA-PDA precursor, 88.7 Å for the PMDA-PDA precursor, and 41.2 Å for the BPDA-ODA precursor. That is, the chain rigidity is in the increasing order BPDA-ODA < BPDA-PDA < PMDA-PDA. These chain rigidities are directly related to the $T_g$ values. In comparison, the PMDA-PDA precursor with the highest chain rigidity exhibits the highest $T_g$,
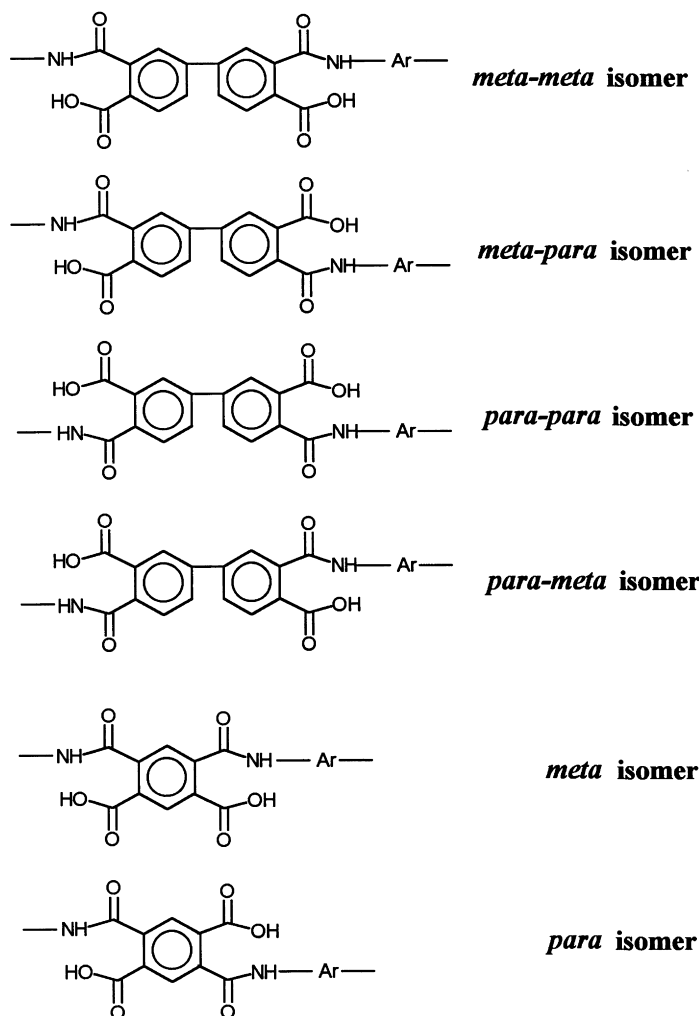
**Figure 11** Possible isomeric repeat units in BPDA-PDA, BPDA-ODA, and PMDA-PDA precursors: Ar denotes PDA or ODA unit

**Table 6** Kuhn statistical segments ($L_K$ values) with their parameters and glass transition temperatures ($T_g$ values) of several poly(amic acid)s and polyamides

| Polymers | $v$ | $\langle h^2 \rangle/n$ (Å$^2$) | $\lambda$ (Å) | $L_K$ (Å) | $T_g^a$ (K) |
|---|---|---|---|---|---|
| Precursors | | | | | |
| BPDA-PDA | 4 | 3664.6 | 58.9 | 62.2 | 521.6 |
| PMDA-PDA | 1 | 1966.1 | 22.2 | 88.7 | 556.6 |
| BPDA-ODA | 8 | 3225.7 | 78.3 | 41.2 | 457.6 |
| Polyamides | | | | | |
| i-PHA-BDA | 1 | 867.0 | 14.7 | 58.9 | 558.0 |
| i-PHA-PDA | 1 | 491.5 | 11.1 | 44.3 | 500.0 |
| i-PHA-ODA | 1 | 253.9 | 8.0 | 31.9 | 463.0 |

$^a$ Glass transition temperatures of polymers in solvent free



**Figure 12** Relationships of Kuhn statistical segments ($L_K$ values) and glass transition temperatures ($T_g$ values) obtained for several aromatic poly(amic acid)s and polyamides

556.6 K (283.4°C), whereas the BPDA-ODA precursor with the lowest chain rigidity reveals the lowest $T_g$, 457.6 K (184.4°C). The BPDA-PDA precursor with an intermediate chain rigidity shows an intermediate $T_g$, 521.6 K (248.4°C).

The poly(amic acid)s studied in the present work can be classified into aromatic polyamides, because of their amide bond-based backbones. Thus, it is valuable to compare the determined chain rigidities and $T_g$ values to those of aromatic polyamides, which have backbone structures similar to the precursor polymers, respectively. Here, three aromatic polyamides were considered in which $T_g$ values were previously reported in the literature[70–72]: poly(4,4′-biphenylene isophthalamide) (i-PHA-BDA),
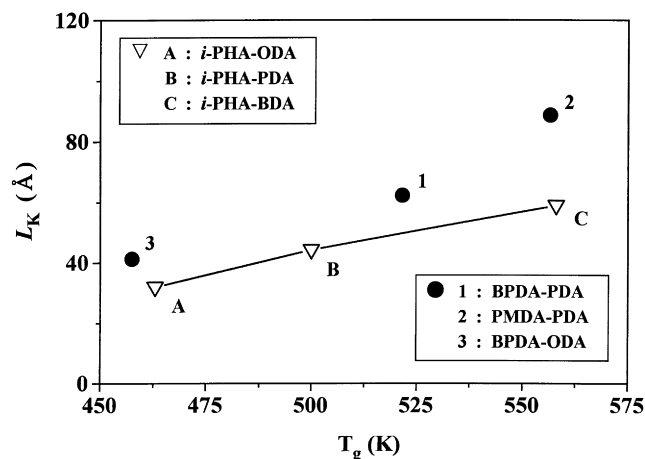
poly(*p*-phenylene isophthalamide) (i-PHA-PDA), and poly(4,4-oxydiphenylene isophthalamide) (i-PHA-ODA). For these polyamides, Kuhn statistical segments were calculated in the same manner as described for the precursors. The calculated Kuhn statistical segments are compared with those of the precursors in *Table 6* and

*Figure 12*. i-PHA-BDA exhibits 58.9 Å $L_K$ and 558 K (285°C), whereas i-PHA-ODA reveals 31.9 Å $L_K$ and 463 K (190°C). i-PHA-PDA shows 44.3 Å $L_K$ and 500 K (227°C). For these polyamides, higher chain rigidity gives higher $T_g$. In comparison, i-PHA-BDA exhibits a chain rigidity slightly lower than that of BPDA-PDA precursor, but reveals higher $T_g$ than that of BPDA-PDA by 36.4°C. The $T_g$ of i-PHA-BDA is comparable with that of PMDA-PDA which has relatively much higher chain rigidity. i-PHA-ODA shows a chain rigidity lower than that of BPDA-ODA and, however, its $T_g$ is slightly higher. i-PHA-PDA has a chain rigidity slightly higher than that of BPDA-ODA by only 3.1 Å, but its $T_g$ is higher than that of BPDA-ODA by 42.4°C. Overall, the poly(amic acid) precursors studied here exhibited relatively lower $T_g$ than those of the polyamides considered, in spite of their relatively high chain rigidities. This result may result from two reasons in the following: First, all the poly(amic acid)s have two orthocarboxylic acid groups per a repeat unit, as side-groups. The side groups may cause a reduction of $T_g$. Second, the chain rigidities, which were calculated under the assumption that the precursors consist of their possible isomeric repeat units in the alternative manner, may be overestimated.

## CONCLUSIONS

Three poly(amic acid) precursors were synthesized in aprotic NMP solvent from pairs of aromatic dianhydrides and diamines: BPDA-PDA, BPDA-ODA, and PMDA-PDA precursors. The precursor solutions were cast and then dried at various conditions. The amounts of residual NMP solvent in the dried precursor samples were determined by proton n.m.r. spectroscopy to be 25.8–88.3 wt.%, depending on the drying conditions. It is confirmed again in this study that the removal of all the NMP solvent from the cast poly(amic acid) samples is impossible because of the complexation between the solvent molecule and the orthoamic acid of the repeat unit in the precursors. From the n.m.r. spectroscopic results for the highly dried precursor samples, it is suggested that the chemical repeat unit in a poly(amic acid) complexes with 1.46–2.16 NMP molecules, depending on the precursors.

For samples of the poly(amic acid)s dried at various conditions, $T_g$ values were successfully measured by the new oscillating d.s.c. technique, which was recently developed, as a function of the content of residual NMP solvent. Furthermore, for the precursor/NMP mixtures, phase diagrams were constructed from the $T_g$ values measured with varying compositions. In addition, $T_g$ values of the precursors in solvent free (namely, true $T_g$ values of the precursors) were estimated by fitting the measured $T_g$ values by a modified Gordon–Taylor equation as a function of composition: 248.4°C for BPDA-PDA, 283.4°C for PMDA-PDA, and 184.4°C for BPDA-ODA precursor.

The Kuhn statistical segment, which is a measure of chain rigidity, was calculated for the precursor polymers as well as some selected polyamides which have backbone structures similar to the precursors. Overall, higher chain rigidity causes higher $T_g$ for both the precursors and the polyamides. In comparison to the polyamides, the precursors exhibited relatively low $T_g$ values in spite of the relatively high chain rigidities. This may result from two reasons: (i) the orthocarboxylic acid groups in the precursors may reduce $T_g$ values; and (ii) the chain rigidities calculated in the precursors may be overestimated.

## REFERENCES

1. Sroog, C.E., *Prog. Polym. Sci.*, 1991, **16**, 561.
2. Ghosh, K. L. and Mittal, K. L., ed., *Polyimides: Fundamentals and Applications*. Dekker, New York, 1996.
3. Labadie, J., Lee, H., Boese, D., Yoon, D.Y., Volksen, W., Brock, P., Cheng, Y.Y., Ree, M. and Chen, K.R., *Proc. Elect. Comp. Technol. (IEEE)*, 1993, **43**, 327.
4. Czornyj, G., Chen, K.J., Prada-Silva, G., Arnold, A., Souleotis, H.A., Kim, S., Ree, M., Volksen, W., Dawson, D. and DiPietro, R., *Proc. Elect. Comp. Technol. (IEEE)*, 1992, **42**, 682.
5. Deutsch, A., Swaminathan, M., Ree, M., Surovic, C., Arjavalingam, G., Prasad, K., McHoerron, D.C., McAllister, M., Kopcsay, G.V., Giri, A.P., Perfecto, E. and White, G.E., *IEEE Trans. Comp. Packag. Manuf. Technol.: Part B: Adv. Packaging*, 1994, **17**(4), 486.
6. Edwards, W. M. and Robinson, I. M., US Pat. No. 2,867,609, 1959.
7. Sasaki, Y., Inoue, H., Nagi, Y. and Sakai, K., US Pat. No. 4,473,523, 1984.
8. Ree, M., Rojstaczer, S., Yoon, D.Y. and Volksen, W., *J. Polym., Sci.: Part B: Polym. Phys.*, 1992, **30**, 133.
9. Ree, M., Kim, K., Woo, S.H. and Chang, H., *J. Appl. Phys.*, 1996, **81**, 698.
10. Kreuz, J.A., Endrey, A.L., Gay, F.P. and Sroog, C.E., *J. Polym. Sci.: Part A-1*, 1966, **4**, 2607.
11. Ree, M., Yoon, D. Y. and Volksen, W., *J. Polym. Sci.: Part B: Polym. Phys.*, 1991, **29**, 1203; *Polym. Mat. Sci. Eng. (ACS)*, 1989, **60**, 179.
12. Bell, V.L. and Jewell, R.A., *J. Polym. Sci.: Part A-1*, 1967, **5**, 3043.
13. Ree, M., Swanson, S. A., Volksen, W. and Yoon, D. Y., US Pat. No. 4,954,578, 1990.
14. Ree, M., Yoon, D.Y. and Volksen, W., *Polym. Prepr. (ACS)*, 1990, **31**(1), 613.
15. Ree, M., Swanson, S.A. and Volksen, W., *Polymer*, 1993, **34**, 1423.
16. Ree, M., Volksen, W. and Yoon, D. Y., US Pat. No. 5,302,851, 1994.
17. Kim, K., Ryou, J.H., Kim, Y., Ree, M. and Chang, T., *Polym. Bull.*, 1995, **34**, 219.
18. Ueda, M. and Mori, H., *Makromol. Chem.*, 1993, **194**, 511.
19. Houlihan, F.M., Bachman, B.J., Wilkins, C.W. and Pryde, C.A., *Macromolecules*, 1989, **22**, 4477.
20. Oishi, Y., Kakimoto, M. and Imai, Y., *Polym. Prepr. Jpn.*, 1987, **36**, 315.
21. Greber, G. and Lohmann, D., *Angew. Chem. Intern. Ed.*, 1969, **8**, 899.
22. Harris, F.W., Pamidimukolas, A., Gupta, R., Das, S., Wu, T. and Mock, G., *J. Macromol. Sci. Chem.*, 1984, **A21**, 1117.
23. Unroe, M.R., Reinhardt, B.A. and Arnold, F.E., *Polym. Prepr. (ACS)*, 1985, **26**, 136.
24. Ree, M. and Yoon, D.Y., *Adv. Chem. Ser.*, 1994, **239**, 247.
25. Frost, L.W. and Keese, I.I., *J. Appl. Polym. Sci.*, 1964, **8**, 1039.
26. Vinogradova, S.V., Vygodskii, Ya.S., Vorob'ev, V.D., Churochkina, N.A., Chudina, L.I., Spirina, T.N. and Korshak, V.V., *Vysokomol. Soyed.*, 1974, **A16**(3), 506.
27. Endrey, A. L., US Pat. No. 3,179,630, 1965.
28. Pryde, C.A., *J. Polym. Sci.: Part A: Polym. Chem.*, 1989, **27**, 711.
29. Snyder, R.W. and Sheen, C.W., *Appl. Spect.*, 1988, **42**, 655.
30. Pyun, E., Mathisen, R.J. and Sung, C.S.P., *Macromolecules*, 1989, **22**, 1174.
31. Sacher, E., *J. Macromol. Sci.: Phys.*, 1986, **B25**(4), 405.
32. Ree, M., Woo, S.H., Kim, K., Chang, H., Zin, W.C., Lee, K.-B. and Park, Y.J., *Macromolecular Symposia*, 1997, **118**, 213.
33. Brekner, M.-J. and Feger, C., *J. Polym. Sci.: Part A: Polym. Chem.*, 1987, **25**, 2429.
34. Feger, C., *Polym. Mat. Sci. Eng. (ACS)*, 1988, **59**, 51.
35. Takahashi, N., Yoon, D.Y. and Parrish, W., *Macromolecules*, 1984, **17**, 2583.
36. Molis, S.E., Saraf, R. and Hodgson, R.T., *ANTEC-Conf. Proc.*, 1991, **37**, 1700.
37. Russell, T.P., *J. Polym. Sci.: Part B: Polym. Phys.*, 1984, **22**, 1105.
38. Ree, M., unpublished results.

39. Venditti, R.A. and Gillham, J.K., *Polym. Mat. Sci. Eng. (ACS)*, 1993, **69**, 434.
40. Reading, M., *Trend Polym. Sci.*, 1993, **8**, 248.
41. Jung, D.H., Kwon, T.W., Bae, D.J., Moon, I.K. and Jeong, Y.H., *Meas. Sci. Technol.*, 1992, **3**, 475.
42. Boller, A., Jin, Y. and Wunderlich, B., *J. Therm. Anal.*, 1994, **42**, 307.
43. Schawe, J.E.K., *Thermochim. Acta*, 1995, **261**, 183.
44. Hatta, I., *Thermochim. Acta*, 1996, **272**, 49.
45. Seiko Instrument Inc., TA Application Brief No. 64, 1993.
46. Jenckel, E. and Heusch, R., *Kolloid-Z.*, 1953, **130**, 89.
47. Uemastu, I. and Honda, K., *Reports Prog. Polym. Phys. Jpn.*, 1966, **10**, 245.
48. Swanson, S.A., Cotts, P.M., Siemens, R. and Kim, S.H., *Macromolecules*, 1991, **24**, 1352.
49. Cotts, P.M., *J. Polym. Sci.: Part B: Polym. Phys.*, 1986, **24**, 923.
50. Kargin, V.A., *J. Polym. Sci.: Part C*, 1963, **4**, 1601.
51. Bartenev, G.M. and Kongarov, G.S., *Rubber Chem. Technol.*, 1963, **36**, 668.
52. Fox, T.G., *Bull. Am. Phys. Soc.: Part 2*, 1956, **2**, 123.
53. Gordon, H. and Taylor, T.S., *J. Appl. Chem.*, 1952, **2**, 493.
54. Kelley, F.N. and Bueche, F., *J. Polym. Sci.*, 1961, **50**, 549.
55. Nishi, T. and Wang, T.T., *Macromolecules*, 1975, **8**, 909.
56. Akiyama, S., Komatsu, J. and Kaneko, R., *Polym. J.*, 1975, **7**, 172.
57. Akiyama, S., *Bull. Chem. Soc. Jpn.*, 1972, **45**, 1381.
58. Dimarzio, E.A. and Gibbs, J. H., *J. Polym. Sci.*, 1959, **40**, 121.
59. Kanig, G., *Kolloid-Z.*, 1963, **190**, 1.
60. Wood, L.A., *J. Polym. Sci.*, 1958, **28**, 319.
61. Johnston, N.W., *Macromolecules*, 1973, **6**, 453.
62. Uemastu, I. and Honda, K., *Reports Prog. Polym. Phys. Jpn.*, 1960, **8**, 111.
63. Bondi, A., *J. Phys. Chem.*, 1964, **68**, 441.
64. Slonimskii, G.L., Askadskii, A.A. and Kitaigorodskii, A.I., *Vyskomol. Soedin.*, 1970, **12**, 494.
65. Simha, R. and Boyer, R.F., *J. Chem. Phys.*, 1962, **37**, 1003.
66. Kuhn, W., *Kolloid-Z.*, 1936, **76**, 258.
67. Birshtein, T.M., Zubkov, V.A., Milevskaya, I.S., Eskin, V.E., Baranovskaya, I.A., Koton, M.M., Kudryavtsev, V.V. and Sklizkova, V.P., *Eur. Polym. J.*, 1977, **13**, 375.
68. Birshtein, T.M., *Vyskomol. Soedin.*, 1977, **A19**, 54.
69. Flory, P., *Statical Mechanics of Chain Molecules*. Wiley & Sons, New York, 1969.
70. Frosini, V., Pasquini, M. and Butta, E., *Chim. Ind.*, 1971, **53**, 140.
71. Butta, E., De Petris, S., Frosini, V. and Pasquini, M., *Eur. Polym. J.*, 1971, **7**, 387.
72. Wrasidlo, W. and Augl, J.M., *J. Polym. Sci.: A-1*, 1969, **7**, 321.